

# Nanoscale

Accepted Manuscript



This is an *Accepted Manuscript*, which has been through the Royal Society of Chemistry peer review process and has been accepted for publication.

*Accepted Manuscripts* are published online shortly after acceptance, before technical editing, formatting and proof reading. Using this free service, authors can make their results available to the community, in citable form, before we publish the edited article. We will replace this *Accepted Manuscript* with the edited and formatted *Advance Article* as soon as it is available.

You can find more information about *Accepted Manuscripts* in the [Information for Authors](#).

Please note that technical editing may introduce minor changes to the text and/or graphics, which may alter content. The journal's standard [Terms & Conditions](#) and the [Ethical guidelines](#) still apply. In no event shall the Royal Society of Chemistry be held responsible for any errors or omissions in this *Accepted Manuscript* or any consequences arising from the use of any information it contains.

## COMMUNICATION

# Electrofocusing-Enhanced Localized Surface Plasmon Resonance Biosensors†

Cite this: DOI: 10.1039/x0xx00000x

Jinling Zhang<sup>a, ‡</sup>, Yi Wang<sup>a, ‡</sup>, Ten It Wong<sup>b</sup>, Xiaohu Liu<sup>a</sup>, Xiaodong Zhou<sup>b</sup>, and Bo Liedberg<sup>\*a</sup>Received 00th January 2012,  
Accepted 00th January 2012

DOI: 10.1039/x0xx00000x

www.rsc.org/

**Localized surface plasmon resonance (LSPR) biosensors typically suffer from diffusion limited mass transport and nonspecific adsorption upon detection of biomolecules in real biofluids. We employ here a peptide-modified plasmonic gold nanohole (AuNH) array for real-time detection of human troponin I (cTnI). Applying a negative electric bias on the AuNH sensor chip enables us to attract and concentrate cTnI at the sensor surface, while repelling other proteins thus decreasing interferences due to nonspecific adsorption.**

Surface plasmon resonance (SPR) originates from collective oscillations of the free electron cloud in metals.<sup>1</sup> Due to the high field enhancement and high sensitivity of SPR to the refractive index changes, it has been extensively applied on photo-catalysis,<sup>2-4</sup> optoelectronic devices<sup>5</sup> and biosensors<sup>6-8</sup> based on label-free,<sup>4, 9-11</sup> fluorescence enhancement<sup>12-16</sup> and surface enhanced Raman scattering<sup>17-20</sup>. Label-free SPR biosensors typically provide a limit of detection (LOD) in the 0.1-10 ng/cm<sup>2</sup> regime.<sup>6</sup> There are several key factors limiting the sensitivity of SPR sensors, including 1) the bulk refractive index sensitivity of SPR, 2) the diffusion limited mass transport of the target molecules to the sensor surface which slows down the molecular binding and limits the sensor response, and 3) the high nonspecific adsorption of undesirable molecules on the sensor surface such as albumin in serum samples which might lead to erroneous responses *e.g.* due to blocking of specific binding sites. Several methods have been employed to boost the sensitivity including well-designed nanostructures with improved refractive-index sensitivity,<sup>11</sup> amplification of the SPR signal with nanoparticles<sup>21-24</sup> and enzyme labeling,<sup>25, 26</sup> tuning the pH of samples to minimize the nonspecific adsorption,<sup>27</sup> and applying magnetic field<sup>28, 29</sup> and electric field<sup>30-33</sup> to promote the molecular diffusion. For instance, magnetic fields enabled rapid capture of magnetic nanoparticle-targeted hCG and E.coli bacteria to a grating-coupled

SPR sensor surface.<sup>28, 29</sup> In addition, the electric field applied to a LSPR sensor chip offered a route to control the adsorption of molecules to the sensor surface.<sup>32, 33</sup> Furthermore, the influences of the applied electric field on the LSPR resonance have been discussed,<sup>34-39</sup> and several groups integrated electric biasing or electrochemistry with LSPR for biosensing.<sup>32, 40, 41</sup> However, limited research has been devoted to studies aiming at reducing the nonspecific adsorption of abundant molecules such as serum albumin, an important plasma protein, while enhancing the binding of target molecules to the sensor surface.

Here, we present a combined LSPR electrofocusing platform for the detection of human troponin I (cTnI), a biomarker of myocardial infarction. A gold nanohole (AuNH) array is employed both as the LSPR sensor chip and as the working electrode. The LSPR sensor responses upon binding of cTnI and the nonspecific adsorption of bovine serum albumin (BSA) were investigated on the AuNH substrate under different biases. As the isoelectric point of cTnI (pI = 9.87) is higher than for BSA (pI = 4.7), a negative bias applied on the sensor surface is expected to favour the specific capture of cTnI while repelling BSA molecules from the sensor surface (Fig. 1a). In addition, the bias applied on the substrate creates a high electric field gradient at the edge of the nanohole, thereby offering an efficient mean of capturing molecules at the edge of the nanoholes where the plasmon field provides the highest sensitivity to refractive index changes.<sup>42</sup> Therefore, the sensitivity for selective detection of cTnI is expected to improve significantly under negative biases applied on the sensor chip.

The AuNH array was prepared through a serial of steps involving nickel mold fabrication by electron beam lithography (EBL) and AuNH array production by nano-imprinting (see experimental details in the Supporting Information).<sup>43, 44</sup> An area of 2×2 mm<sup>2</sup> consisting of a layer of 50 nm Au coated on glass with periodic (pitch of 400 nm) holes 140 nm in diameter is located at the center of a chip. The AuNH array was characterized by scanning electron microscopy (SEM), atomic force microscopy (AFM) and UV-vis spectroscopy (UV-vis) (Fig. 1), all indicating a periodic and uniform

hole array. The plasmon resonance peak typically shifts to higher wavelength upon molecular binding to the surface of the nanohole, leading to a decrease of the extinction difference  $Ext_d$  (Fig. 1d). The  $Ext_d$  was obtained from the extinction intensity difference at two wavelengths, e.g.  $\lambda_1$  and  $\lambda_2$  (Fig. 1d). The AuNH array was modified in an 1:1 mixture of a short peptide CALNN and CALNN-(PEG)<sub>4</sub>-FYSHSFHENWPS,<sup>45</sup> a peptide specific for cTnI (see the details in the Supporting Information). Extinction spectra were measured by Xnano instrument (Xnano) and the  $Ext_d$  between two pre-selected wavelengths at about  $\lambda_1 = 700\text{nm}$  and  $\lambda_2 = 730\text{nm}$ , was monitored in real-time (i.e.  $Ext_d(t) = Ext_{730}(t) - Ext_{700}(t)$ ).

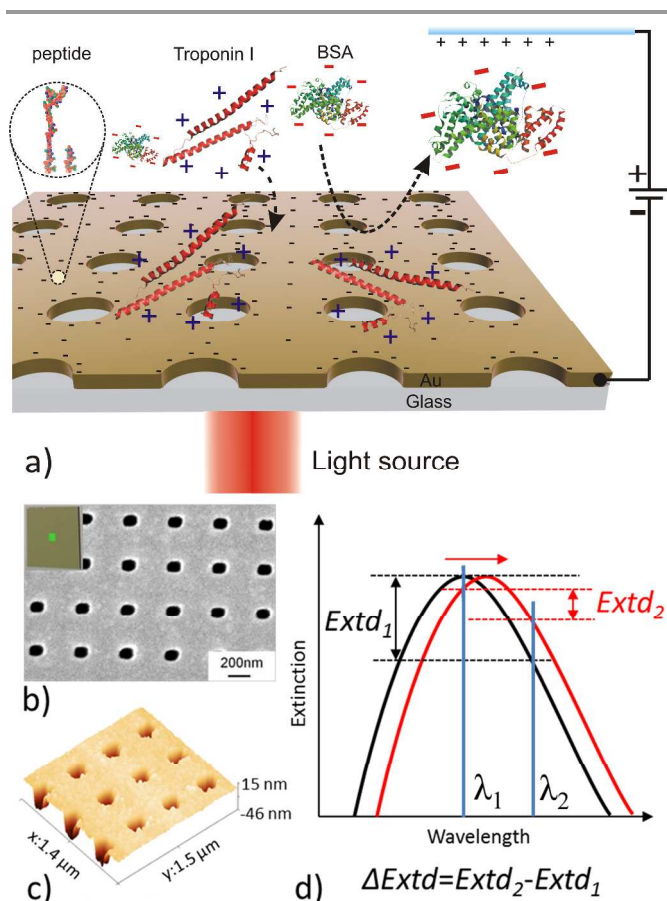


**Fig. 1** a) Schematic illustration of the setup and the modified AuNH array chip applied with a negative bias for minimizing the nonspecific adsorption of BSA and simultaneously attracting the target cTnI to the sensor surface. b) SEM and a photo of the chip (inset). c) AFM image of AuNH array. d) The extinction spectra of AuNH array typically shift to longer wavelength upon molecular binding, leading to decrease of the extinction difference  $Ext_d$  derived from two preselected wavelengths  $\lambda_1$  and  $\lambda_2$ . The change of  $Ext_d$  is defined as  $\Delta Ext_d = Ext_{d2} - Ext_{d1}$ .

In order to investigate the effect of applied electric bias on LSPR response, three cycles of voltage scans (from 0V, 0.6V, -0.6V and back to 0V at a scanning rate of 100 mV/s vs Ag/AgCl electrode) were applied on the peptide-modified AuNH array before and after incubation with cTnI in the PBS buffer (Fig. 2). The  $Ext_d$  value shifted synchronously with the applied bias. Positive bias resulted in an increasing  $Ext_d$  value (less negative), indicating red-shift of the LSPR peak, while negative bias induced a blue-shift (Fig. S1). The

relative magnitude of the observed shifts is attributed to the higher polarizability of the  $\text{Cl}^-$  ion ( $4.17 \text{ \AA}^3$ ) with respect to water molecules ( $1.43 \text{ \AA}^3$ ) and  $\text{Na}^+$  ions ( $0.148 \text{ \AA}^3$ ).<sup>46</sup> According to the DLVO theory, the applied electric field on the surface influences the electric double layer in solution. Different strength of the applied potential results in a redistribution of ions within the double layer, thus varying the refractive index near the surface.<sup>47</sup> Interestingly, the chip after binding with cTnI showed higher  $Ext_d$  changes ( $\Delta Ext_d$ ) under voltage sweeping from 0.6 V to -0.6 V (Fig. 2). This is most likely due to an increase in the effective surface area of the AuNH after the binding of positively charged cTnI molecules (see the AFM imaging in Fig. S2), resulting indirectly to an increasing concentration of highly polarizable  $\text{Cl}^-$  ions near the surface.

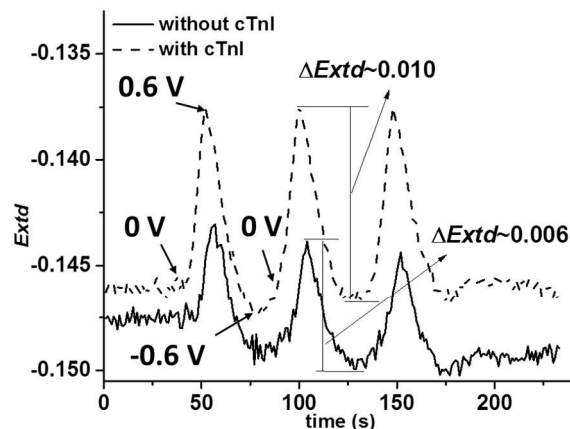


**Fig. 2.** LSPR responses of modified AuNH array under voltage sweeping measured in PBS buffer before (solid line) and after incubation of 3  $\mu\text{g/ml}$  cTnI for 30 min (dashed line). The voltage was swept (three cycles) from 0V, 0.6V, -0.6V and back to 0V at scanning rate of 100 mV/s.

Real-time measurements of the LSPR response upon injection of cTnI (PBS) into the reaction chamber were carried out under different biases applied to the sensor chip (vs Ag/AgCl electrode), as shown in Fig. 3a. The  $\Delta Ext_d$  (with the background  $Ext_d$  offset to zero) slowly increased after the injection of 100 ng/mL cTnI under 0 V bias and the response increased with the concentration of cTnI beyond 100 ng/mL. Control experiment carried out on the sensor chip without the specific peptide modification (only CALNN) revealed negligible nonspecific adsorption (Fig. S3). The  $\Delta Ext_d$  value of each concentration was calculated by subtracting the background value ( $\Delta Ext_d(t < 60\text{min})$ ) from that after 30min incubation. The calibration curve under 0 V (triangles in Fig. 3b) was fitted by a sigmoidal model (Equation S1), and the LOD was estimated to  $\sim 110\text{ ng/mL}$  for our platform under 0 V. The noise level was calculated as 3 times the standard deviation of the  $Ext_d$  before injection of cTnI in the solution.

Assuming the binding events are limited by the mass transport diffusion, the surface coverage of molecules on the sensor surface during the incubation time of  $t$  can be simplified as  $\Gamma = 2C_{\text{bulk}}\sqrt{Dt/\pi}$ ,<sup>33, 48, 49</sup> where  $C_{\text{bulk}}$  is the bulk concentration of analyte in the solution,  $D$  is the diffusion constant of the molecules (see details in the Supporting Information). Based on an LOD of 110 ng/ml achieved for 30-min incubation (0 V), we are able to estimate the smallest detectable surface mass of  $\Gamma_{\text{LOD}} = 2.9\text{ ng/cm}^2$ . Thus our results indicate that it is necessary to allow for 63 days of incubation

to achieve LOD of 2 ng/ml, which is approximately the clinical level of cTnI found in healthy people.

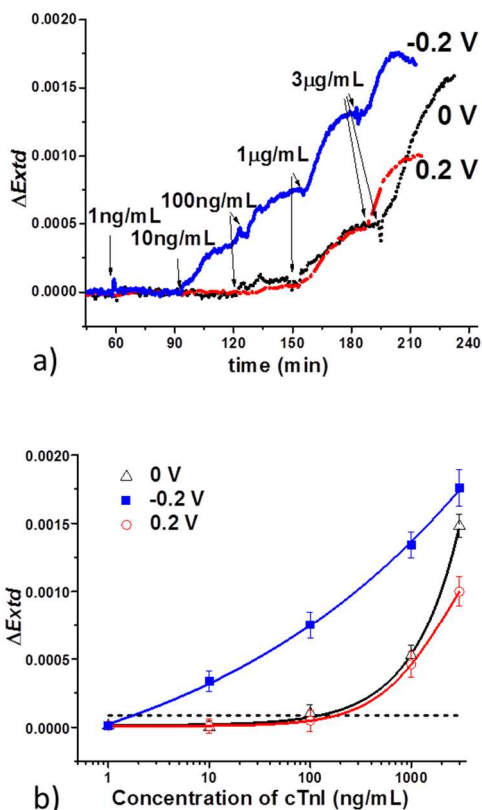


**Fig. 3.** a) Real-time  $\Delta Ext_d$  measured on the AuNH array with a series of injections of cTnI in PBS. Sensor response for 0 V (black curve), -0.2 V (blue curve) and 0.2 V (red curve). b)  $Ext_d$  changes ( $\Delta Ext_d$ ) as function of the cTnI concentration measured under no bias (triangles), -0.2V bias (squares) and 0.2V bias (circles). Dotted line is 3 times of standard deviation.

The binding rate and the sensor response was significantly improved under -0.2 V bias applied to the sensor chip. For instance, the initial binding rate for 10 ng/ml cTnI is comparable to 1  $\mu$ g/ml cTnI under 0 V bias. The LOD is improved by two orders of magnitude to 1.8 ng/ml under -0.2 V bias (Fig. 3b, table 1), for a reaction time of 30 min, which is theoretically more than 3000 times faster than the diffusion limited assay  $t \sim 77.5$  days at 0 V. Positive bias applied on the sensor surface hinders the binding of cTnI to the sensor surface, thereby worsening the LOD to 170 ng/ml (Fig. 3, table 1).

Table 1. Result of AuNH array as sensor under different bias.

Medium	Bias (V)	LOD (ng/mL)
PBS	0	110
	0.2	170
	-0.2	1.8
BSA	0	8*
	-0.2	25**

\* (with 3 mg/ml BSA in PBS)

\*\* (in 10 $\times$  diluted rabbit serum in PBS)

While, the negatively charged molecules such as BSA (pI=4.7) are repelled from the sensor surface the nonspecific adsorption is expected to decrease. For instance, after injection of 3 mg/ml BSA in PBS, the LSPR sensor response due to BSA adsorption decreased by a factor of 2 at -0.2V bias (Fig. S4). To investigate the possibility of detecting cTnI in complex samples at -0.2 V bias, we started by adding various concentrations of cTnI (1 ng/ml to 3  $\mu$ g/ml) in PBS containing 3 mg/ml BSA. The extinction changes were monitored in real time before and after the injection of the cTnI in the BSA containing buffer solutions (Fig. 4a). A slow increase of the  $\Delta Ext_d$  was seen upon the injection of 3 mg/ml BSA. Sequential injections of cTnI revealed a significant response at 100 ng/ml cTnI, and a LOD of about 8 ng/ml was estimated for the detection of cTnI in 3 mg/ml BSA, see insert Fig. 4a and Table 1. This result indicated the feasibility for the detection of cTnI in solution of high BSA concentration, and potentially also for more complex biofluids like serum or plasma.

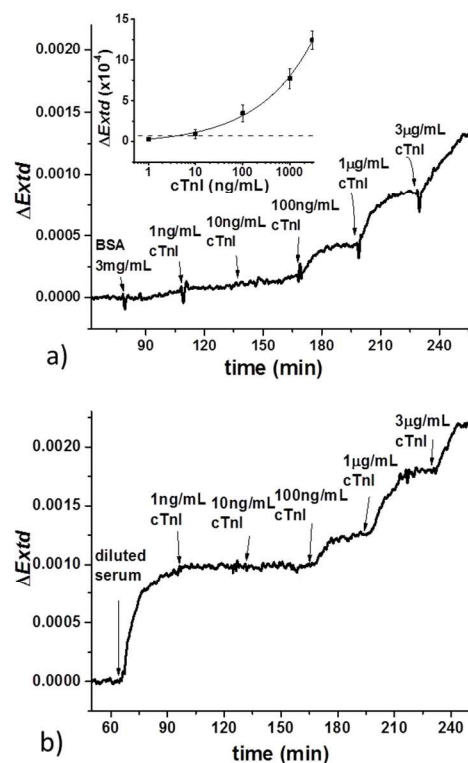


**Fig. 4.** a) Real-time LSPR signals of AuNH array under -0.2V bias. Inset is the calibration curve for the detection of cTnI spiked in PBS with 3 mg/ml BSA under -0.2V bias. b) The real-time  $Ext_d$  changes measured on AuNH array under -0.2 V bias for the detection of cTnI in 10 $\times$  diluted rabbit serum.

The nonspecific adsorption of a 10-time diluted rabbit serum was subsequently investigated (Fig. 4b). The nonspecific adsorption was reduced by a factor of 2 by monitoring the  $\Delta Ext_d$  after applying -0.2 V bias (Fig. S5). However, the response induced by the nonspecific adsorption ( $\Delta Ext_d = 0.001$ ) was still higher than the specific sensor response to 3  $\mu$ g/ml cTnI (Fig. 4b), suggesting that other molecules/proteins than serum albumin (e.g. globulins and antibodies) may adsorb to the sensor surface. In serum, the major protein is serum albumin with concentration of 35-52 mg/ml. Other proteins include globulins (22-40 mg/ml, isoelectric point, pI $\sim$ 7.5),

antibodies (total 5.8-27 mg/ml) and many more at lower concentration.<sup>50</sup> Due to their high concentration and weakly positive charge, nonspecific adsorption induced by globulins, and to some extent also by antibodies, were unavoidable under -0.2 V bias. Nevertheless, the sensor response to cTnI at 100 ng/ml was comparable to that measured in PBS buffer. A LOD of 25 ng/ml was achieved in serum samples (Fig. S6). Control experiments carried out under bias of 0.4 V and -0.4 V indicated a poor long-term stability of the sensor response, which might be ascribed to the dissociation of the thiol molecules from the sensor surface and/or oxidation/chlorination of the gold film. Taken together, electrofocusing at -0.2 V offers a route to reduce non-specific adsorption of negatively charge proteins to the peptide modified AuNH array thereby allowing for detection of cTnI in biofluids of increasing complexity.

## Conclusions

We have successfully demonstrated an electrofocusing-enhanced plasmonic sensor based on a gold nanohole array for the detection of cTnI in buffer, BSA solution and rabbit serum. The limit of detection (LOD) in buffer can be improved by ~2 orders of magnitude upon changing from 0 to -0.2 V bias applied to the sensor surface. The nonspecific adsorption of serum albumin (*i.e.* BSA) and rabbit serum is also reduced at -0.2 V. This method provides an avenue for highly sensitive detection of biomolecules in complex fluids like serum without tedious sample purification and pretreatment.

## Acknowledgement

This research is supported by Science & Engineering Research Council (SERC) of Agency for Science, Technology and Research (A\*STAR), for projects under the numbers of 102 152 0014 and 102 152 0015. The authors acknowledge support from School of Materials Science and Engineering and Provost Office of NTU.

## Notes and references

<sup>a</sup> Centre for Biomimetic Sensor Science, School of Materials Science and Engineering, Nanyang Technological University, 50 Nanyang Drive, Singapore 637553. E-mail: bliedberg@ntu.edu.sg, yiwang@ntu.edu.sg

<sup>b</sup> Institute of Materials Research and Engineering, Agency for Science, Technology and Research (A\*STAR), 3 Research Link, Singapore 117602.

† Electronic Supplementary Information (ESI) available: [details of any supplementary information available should be included here]. See DOI: 10.1039/c000000x/

‡ These authors contributed equally to this work.

- E. Altewischer, M. P. van Exter and J. P. Woerdman, *Nature*, 2002, **418**, 304-306.
- S. Lincic, P. Christopher and D. B. Ingram, *Nat. Mater.*, 2011, **10**, 911-921.
- S. C. Warren and E. Thimsen, *Energy Environ. Sci.*, 2012, **5**, 5133-5146.
- X. Huang, Y. Li, Y. Chen, H. Zhou, X. Duan and Y. Huang, *Angew. Chem. Int. Ed.*, 2013, **52**, 6063-6067.
- Q. Gan, F. J. Bartoli and Z. H. Kafafi, *Adv. Mater.*, 2013, **25**, 2385-2396.
- J. Homola, *Chem. Rev.*, 2008, **108**, 462-493.
- X. Liu, Y. Wang, P. Chen, Y. Wang, J. Mang, D. Aili and B. Liedberg, *Anal. Chem.*, 2014, **86**, 2345-2352.
- Y. Wang, X. Liu, J. Zhang, D. Aili and B. Liedberg, *Chem. Sci.*, 2014, **5**, 2651-2656.
- L. J. Sherry, S. H. Chang, G. C. Schatz, R. P. Van Duyne, B. J. Wiley and Y. N. Xia, *Nano Lett.*, 2005, **5**, 2034-2038.
- G. Raschke, S. Kowarik, T. Franzl, C. Sonnichsen, T. A. Klar, J. Feldmann, A. Nichtl and K. Kurzinger, *Nano Lett.*, 2003, **3**, 935-938.
- K. M. Mayer and J. H. Hafner, *Chem. Rev.*, 2011, **111**, 3828-3857.
- A. Kinkhabwala, Z. Yu, S. Fan, Y. Avlasevich, K. Muellen and W. E. Moerner, *Nat. Photonics*, 2009, **3**, 654-657.
- J. R. Lakowicz, K. Ray, M. Chowdhury, H. Szmajdzinski, Y. Fu, J. Zhang and K. Nowaczyk, *Analyst*, 2008, **133**, 1308-1346.
- D. Punj, M. Mivelle, S. B. Moparthi, T. S. van Zanten, H. Rigneault, N. F. van Hulst, M. F. Garcia-Parajo and J. Wenger, *Nat. Nanotechnol.*, 2013, **8**, 512-516.
- Y. Wang, A. Brunsen, U. Jonas, J. Dostalek and W. Knoll, *Anal. Chem.*, 2009, **81**, 9625-9632.
- Y. Wang, J. Dostalek and W. Knoll, *Biosens. Bioelectron.*, 2009, **24**, 2264-2267.
- M. D. Porter, R. J. Lipert, L. M. Siperko, G. Wang and R. Narayana, *Chem. Soc. Rev.*, 2008, **37**, 1001-1011.
- P. Chen, Z. Yin, X. Huang, S. Wu, B. Liedberg and H. Zhang, *J. Phys. Chem. C*, 2011, **115**, 24080-24084.
- Y. Zhang, J. Qian, D. Wang, Y. Wang and S. He, *Angew. Chem. Int. Ed.*, 2013, **52**, 1148-1151.
- S. Schluecker, *Angew. Chem. Int. Ed.*, 2014, **53**, 4756-4795.
- M. Frascioni, C. Tortolini, F. Botre and F. Mazzei, *Anal. Chem.*, 2010, **82**, 7335-7342.
- L. He, M. D. Musick, S. R. Nicewarner, F. G. Salinas, S. J. Benkovic, M. J. Natan and C. D. Keating, *J. Am. Chem. Soc.*, 2000, **122**, 9071-9077.
- S. Krishnan, V. Mani, D. Wasalathanthri, C. V. Kumar and J. F. Rusling, *Angew. Chem. Int. Ed.*, 2011, **50**, 1175-1178.
- A. W. Wark, H. J. Lee, A. J. Qavi and R. M. Corn, *Anal. Chem.*, 2007, **79**, 6697-6701.
- T. T. Goodrich, H. J. Lee and R. M. Corn, *J. Am. Chem. Soc.*, 2004, **126**, 4086-4087.
- H. J. Lee, Y. Li, A. W. Wark and R. M. Corn, *Anal. Chem.*, 2005, **77**, 5096-5100.
- H. M. Lou, J. Y. Zhu, T. Q. Lan, H. R. Lai and X. Q. Qiu, *Chemosuschem*, 2013, **6**, 919-927.
- Y. Wang, J. Dostalek and W. Knoll, *Anal. Chem.*, 2011, **83**, 6202-6207.
- Y. Wang, W. Knoll and J. Dostalek, *Anal. Chem.*, 2012, **84**, 8345-8350.
- E. C. Lin, J. Fang, S. C. Park, F. W. Johnson and H. O. Jacobs, *Nat. Commun.*, 2013, **4**.
- E.-C. Lin, J. Fang, S.-C. Park, T. Stauden, J. Pezoldt and H. O. Jacobs, *Adv. Mater.*, 2013, **25**, 3554-3559.
- D. Pallarola, M. Schneckenburger, J. P. Spatz and C. Pacholski, *Chem. Commun.*, 2013, **49**, 8326-8328.
- A. Barik, L. M. Otto, D. Yoo, J. Jose, T. W. Johnson and S.-H. Oh, *Nano Lett.*, 2014, **14**, 2006-2012.
- A. B. Dahlin, T. Sannomiya, R. Zahn, G. A. Sotiriou and J. Voeroes, *Nano Lett.*, 2011, **11**, 1337-1343.
- K. J. Foley, X. Shan and N. J. Tao, *Anal. Chem.*, 2008, **80**, 5146-5151.
- C. Novo and P. Mulvaney, *Nano Lett.*, 2007, **7**, 520-524.
- T. Sannomiya, H. Dermutz, C. Hafner, J. Voeroes and A. B. Dahlin, *Langmuir*, 2010, **26**, 7619-7626.
- X. Shan, U. Patel, S. Wang, R. Iglesias and N. Tao, *Science*, 2010, **327**, 1363-1366.
- S. Wang, X. Huang, X. Shan, K. J. Foley and N. Tao, *Anal. Chem.*, 2010, **82**, 935-941.
- X. R. Cheng, B. Y. H. Hau, T. Endo and K. Kerman, *Biosens. Bioelectron.*, 2014, **53**, 513-518.
- T. G. Drummond, M. G. Hill and J. K. Barton, *Nat. Biotechnol.*, 2003, **21**, 1192-1199.
- T. Sannomiya, O. Scholder, K. Jefimovs, C. Hafner and A. B. Dahlin, *Small*, 2011, **7**, 1653-1663.
- Y. Wang, L. Wu, X. D. Zhou, T. I. Wong, J. L. Zhang, P. Bai, E. P. Li and B. Liedberg, *Sensor. Actuat. B-Chem.*, 2013, **186**, 205-211.
- T. I. Wong, S. Han, L. Wu, Y. Wang, J. Deng, C. Y. L. Tan, P. Bai, Y. C. Loke, X. D. Yang, M. S. Tse, S. H. Ng and X. Zhou, *Lab Chip*, 2013, **13**, 2405-2413.
- J. P. Park, D. M. Cropek and S. Banta, *Biotechnol. Bioeng.*, 2010, **105**, 678-686.
- E. A. Mason and E. W. McDaniel, in *Transport Properties of Ions in Gases*, Wiley-VCH Verlag GmbH & Co. KGaA, 2005, pp. 531-539.
- A. B. Dahlin, B. Dielacher, P. Rajendran, K. Sugihara, T. Sannomiya, M. Zenobi-Wong and J. Voros, *Anal. Bioanal. Chem.*, 2012, **402**, 1773-1784.

## Journal Name

48. D. B. Hibbert, J. J. Gooding and P. Erokhin, *Langmuir*, 2002, **18**, 1770-1776.
49. A. B. Dahlin, *Plasmonic biosensors: an integrated view of refractometric detection*, Ios Press, 2012.
50. D. Weatherby and S. Ferguson, *Blood chemistry and cbc analysis : clinical laboratory testing from a functional perspective*, Vis Medicatrix Press, Jacksonville, OR, 2004.